




Examination of decay heat measurements and their relevance for understanding the origin of the reactor antineutrino anomaly

A. A. Sonzogni ^{1,*}, R. J. Lorek ², A. Mattera ² and E. A. McCutchan²

¹*Nuclear Science & Technology Department, Brookhaven National Laboratory, Upton, New York 11973-5000, USA*

²*National Nuclear Data Center, Brookhaven National Laboratory, Upton, New York 11973-5000, USA*



(Received 24 February 2022; revised 2 June 2023; accepted 8 August 2023; published 31 August 2023)

Measurements of the decay energy released as a function of time following the thermal neutron induced fission of ^{235}U and $^{239,241}\text{Pu}$ were performed in the 1970s at Oak Ridge National Laboratory with the purpose of quantifying possible loss of coolant accident scenarios. The derivative of this decay energy with respect to time, known in technical parlance as decay heat, is mainly composed of two terms, that of the electrons produced together with antineutrinos in the β -minus decay of the neutron-rich fission products, and that of the γ rays produced in the subsequent decay of excited nuclear levels. In this work we study if this extensive set of decay energy measurements can be used to assess the reactor antineutrino anomaly, that is, the approximately 5% deficit of electron antineutrinos produced by nuclear reactors, first deduced by Mention and collaborators in 2011, and observed by the major reactor antineutrino experiments since. With the assistance of nuclear databases, we are able to obtain the ratio of electron spectra under equilibrium conditions for ^{235}U to ^{239}Pu , in better agreement with the lower trend recently reported by Kopeikin and collaborators, as well as those for ^{235}U to ^{241}Pu and ^{241}Pu to ^{239}Pu , which do not agree well with those measured at the Institut Laue-Langevin in the 1980s. We conclude that a new experimental campaign is needed to measure the electron spectra utilizing a high resolution and signal-to-noise-ratio electron spectrometer and a highly precise fission normalization procedure.

DOI: [10.1103/PhysRevC.108.024617](https://doi.org/10.1103/PhysRevC.108.024617)

I. INTRODUCTION

We have witnessed remarkable developments in the field of nuclear reactor antineutrinos in the last ten years, starting with the more precise spectra estimates of Huber [1] and Mueller *et al.* [2]; as well as the detailed analysis of Mention *et al.* [3], which led to the conclusion that approximately 5% of the electron antineutrinos are missing at short distances, a feature that has been coined as the reactor antineutrino anomaly (RAA). On the experimental side, the Daya Bay [4], Double Chooz [5], and RENO [6] collaborations have measured the θ_{13} mixing angle with great precision; they have also revealed a deficit of antineutrinos at the peak of the inverse beta decay (IBD) antineutrino spectrum and a small excess at around 5 MeV with respect to the Huber-Mueller model, also observed by the short-distance NEOS experiment [7]. More recently, the short-distance PROSPECT [9] and STEREO [8] collaborations have published their measured ^{235}U spectra, while PROSPECT-Daya Bay [10] and PROSPECT-STEREO [11] joint analyses were just published. Finally, the results of the long-baseline JUNO experiment [12] are eagerly anticipated by the community.

In order to precisely account for the electron antineutrinos produced by nuclear reactors, we need to have accurate predictions of the antineutrino spectra produced by each of the main nuclides undergoing fission, $^{235,238}\text{U}$ and $^{239,241}\text{Pu}$. Our current best numerical estimates of the ^{235}U and $^{239,241}\text{Pu}$

antineutrino spectra are obtained from a multiaverage- β -decay-branch fit performed by Huber [1] to the corresponding electron spectra measured at the Institut Laue-Langevin (ILL) in the 1980s [13–15]. These electron spectra were measured using the BILL spectrometer, which provided excellent energy resolution and signal-to-noise ratio, from foils placed inside the ILL reactor. For ^{238}U , the summation calculation from Mueller *et al.* [2] is currently considered its best antineutrino spectrum estimate. A number of hypothesis have been postulated to explain the disagreement between the latest reactor spectrum measurements with the Huber-Mueller model, including forbidden β -minus transitions effects [16] and incomplete β -minus decay schemes [17], to name just a few. In this work we explore in detail some of the ILL measurements' underpinnings to find a possible explanation of the RAA, including a comparison with data originally taken to quantify decay heat.

II. ILL SPECTRUM NORMALIZATION

An early indication about possible issues in the ^{235}U ILL data came from Daya Bay's measurement of the IBD antineutrino yield as function of the ^{239}Pu fission fraction [18], which concluded that faulty modeling was responsible for the RAA since their deduced ^{239}Pu IBD yield was in agreement with Huber's value, while the ^{235}U IBD yield was not. The Daya Bay collaboration would later obtain ^{235}U and ^{239}Pu spectra, by themselves [19] and jointly with PROSPECT [10], reaching similar conclusions.

*sonzogni@bnl.gov

For the normalization of the ILL electron spectra, that is, the derivation of absolute number of electrons at a given energy per unit energy per fission, a precise value of the neutron flux inside the reactor was needed, which was obtained by measuring the intensity of selected conversion electrons. From the brief technical description in the ILL articles, we know that the ^{235}U experiment employed conversion electrons following neutron capture on ^{115}In and ^{207}Pb ; the ^{239}Pu one following neutron capture on ^{115}In and ^{197}Au ; and the ^{241}Pu one following neutron capture on ^{113}Cd , ^{115}In , and ^{207}Pb . We have checked all the cross section and conversion coefficient values quoted in the ILL normalization procedure, concluding that they are fairly close to the currently accepted best values, with the exception of the ^{207}Pb thermal neutron capture cross section $\sigma_{n\gamma}(^{207}\text{Pb})$. The ILL group used a $\sigma_{n\gamma}(^{207}\text{Pb})$ value equal to 712 ± 10 mb from the 1981 cross section evaluation work of Mughabghab [20]. This value originates from a 1963 conference proceeding [21], where a $\sigma_{n\gamma}(^{207}\text{Pb})$ value of 709 ± 10 mb was deduced from (i) a natural Pb cross section of 171 ± 2 mb [22], (ii) cross section ratio values $\sigma_{n\gamma}(^{204}\text{Pb})/\sigma_{n\gamma}(^{207}\text{Pb}) = 0.94 \pm 0.07$ and $\sigma_{n\gamma}(^{206}\text{Pb})/\sigma_{n\gamma}(^{207}\text{Pb}) = 0.043 \pm 0.001$ [21]. The latest 2018 evaluation by Mughabghab [23] gives a $\sigma_{n\gamma}(^{207}\text{Pb})$ value of 647 ± 9 mb, that is, 9% lower, since it likely incorporates the results of two experiments that studied the neutron capture of ^{207}Pb in detail, $\sigma_{n\gamma}(^{207}\text{Pb}) = 610 \pm 30$ mb from Blackmon *et al.* [24], and $\sigma_{n\gamma}(^{207}\text{Pb}) = 649 \pm 14$ mb from Schillebeecx *et al.* [25]. It is impossible for us to gauge the quantitative impact of using a larger $\sigma_{n\gamma}(^{207}\text{Pb})$; however, qualitatively this would result in a smaller derived neutron flux, leading to an artificially larger ^{235}U spectrum, thus being a possible explanation for the RAA.

An earlier analysis of the nuclear data involved in the ILL data normalization by Letourneau and Onillon was presented at the 2018 Applied Antineutrino Physics Workshop [26]. In this work, they identified discrepancies between the JEFF-3.1 [27] and JEFF-3.3 [28] $\sigma_{n\gamma}(^{207}\text{Pb})$, which can be traced back to the use of the 1981 and 2005 thermal cross-sections evaluations by Mughabghab [20,29], respectively. They also pointed out an issue with the ^{208}Pb 7.368 MeV E1 γ -ray K conversion coefficient using the BRICC code [30]; we note that the current BRICC tables have a 6 MeV upper limit, and our extrapolated value for the 7.368 MeV γ ray agrees with the one used by ILL.

In the following section we will briefly discuss the recently published work by Kopeikin *et al.* [31], which illustrates the normalization issues in the ILL measurements. This will be followed by a thorough analysis of electron spectra data measured at Oak Ridge National Laboratory in the 1970s, which can provide additional insights into the origin of the RAA. Finally, we succinctly discuss possible experimental approaches to measure well normalized electron spectra under equilibrium conditions which would be used to obtain the corresponding antineutrino ones.

III. KURCHATOV INSTITUTE MEASUREMENTS

Kopeikin *et al.* [31] recently published a measurement of the ^{235}U to ^{239}Pu electron spectra ratio (R_{59}), which is

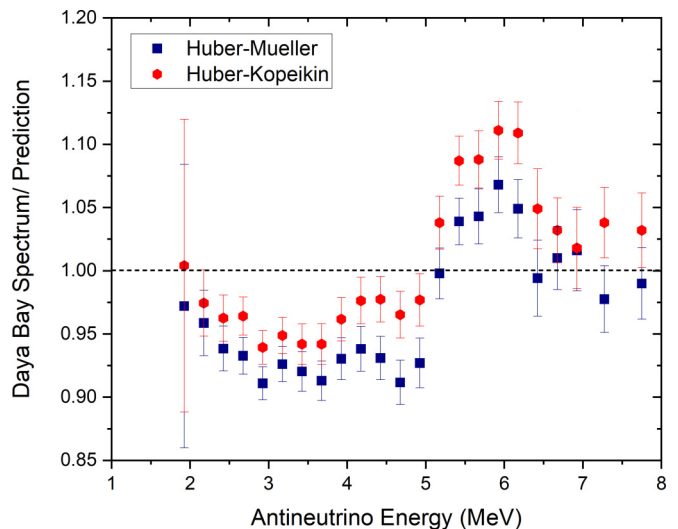


FIG. 1. Ratio of the antineutrino spectrum measured by the Daya Bay collaboration to the Huber-Mueller and Huber-Kopeikin models.

approximately 5% lower than the one obtained from the ILL measurements. In their work, ^{235}U and ^{239}Pu foils were placed outside the Kurchatov Institute (KI) reactor core and electrons were detected using plastic scintillators. Succinctly, Kopeikin *et al.* [31] showed that if ILL's ^{235}U electron spectrum is reduced by 5%, then a much better agreement with Daya Bay's IBD antineutrino yields is achieved, thus possibly eliminating the RAA altogether. This groundbreaking work assumes, however, that the ^{239}Pu and ^{241}Pu normalizations are paradoxically correct, even though the ^{235}U spectrum measured by the same group is not, despite the latter's smaller relative uncertainties and finer energy bin. Additionally, both the ILL and KI R_{59} values unexpectedly drop to nearly unity for energies larger than 8 MeV, a behavior not relevant for the RAA, but nevertheless disquieting as there is no discernible physical reason for the ^{235}U and ^{239}Pu spectra to have similar values at those energies despite that at lower energies the ^{235}U spectrum is considerably larger, hence evidencing possible underlying measurement deficiencies.

Finally, a simple renormalization of the ^{235}U spectrum may not be enough to solve the RAA as can be seen in Fig. 1, which shows the ratio of the 2022 Daya Bay antineutrino data [32] to the usual Huber-Mueller model as well as what we call the Huber-Kopeikin (HK) model, which uses the $^{239,241}\text{Pu}$ Huber antineutrino spectra and Kopeikin's $^{235,238}\text{U}$ ones as listed in the table of Ref. [31] and assuming a linear interpolation between the energy points. As can be seen from this plot, neither the deficit at the IBD spectrum peak, which is the source of the RAA, nor the excess at around 5.5 MeV, known colloquially as the bump are solved with Kopeikin's $^{235,238}\text{U}$ spectra values.

IV. ORNL MEASUREMENTS

We have recently encountered electron spectra from experiments performed at Oak Ridge National Laboratory (ORNL) in the 1970s to properly quantify the decay energy released as

function of time following the thermal neutron-induced fission of ^{235}U [33,34], ^{239}Pu [35], and ^{241}Pu [36] targets. These experiments were performed by a group led by Dickens [37] and were part of a campaign to understand loss of coolant accident scenarios [38,39]. Target foils were irradiated inside the Oak Ridge Research Reactor and later placed in front of a detection system using a rabbit mechanism. Gamma and electron spectra were measured using scintillator detectors, which were normalized per fission by using well-known fission products' γ -decay intensities. Electron spectra for ^{20}F and ^{56}Mn were measured separately, which agreed quite well with calculated ones using nuclear databases, adding an important element of confidence to their experimental results. The electron data for energies above 1.5 MeV are well accounted for by summation calculations; for lower energies, the electron spectra contain contributions from γ rays and conversion electrons.

The data in these reports correspond to three irradiations: a short 1-s one, a medium one of 5 or 10 s, and a long one of 50 or 100 s. The time interval between the irradiation and start of counting, T_{cs} , was 1.7 s for the short irradiation, 10.7 or 17.7 s for the medium ones, and 170 or 250 s for the long ones. Data were counted for 110–130 s, 795–1,198 s, and 13500–14000 s for the three irradiations, respectively. The reports contain 13–15 spectra per irradiation, corresponding to an increasing counting interval to maintain an approximately similar number of counts in the lower-energy portion of the spectra. These reports were submitted to the Nuclear Science References database [40], and the data were submitted to the EXFOR database [41] following their digitization. We note that the ^{235}U and ^{239}Pu β -decay heat values derived from the ORNL data agree well with those measured by Akiyama and San [42,43]; and interestingly, the electron data for ^{235}U , obtained by adding up all the individual electron spectra for the short irradiation, were used to obtain the corresponding equilibrium antineutrino spectrum in 1981 [44], a work which despite its pioneering relevance has not been cited by the many reactor antineutrino articles published in the last ten years, and which agrees surprisingly well with the Huber values, as shown in Fig. 2, despite the 30-year time lapse between them.

Due to the relative similarities between the ORNL experimental setup and Kopeikin's, our goal would be to determine if we can obtain equilibrium spectra ratios from the ORNL data to elucidate possible normalization issues in the ILL electron spectra, despite that none of the irradiation conditions correspond to an equilibrium situation.

V. FORMALISM

Using the summation method [45–48], the electron and antineutrino spectra from a target a under equilibrium conditions can be calculated as

$$S_{s,eq}^a = \sum CFY_j^a S_j, \quad (1)$$

where CFY_j^a are the cumulative fission yields and S_j the corresponding electron or antineutrino spectra. Due to the linear dependence on CFY s, we can convert a spectrum measured with irradiation conditions labeled with the index i , $S_{m,i}^a$, to

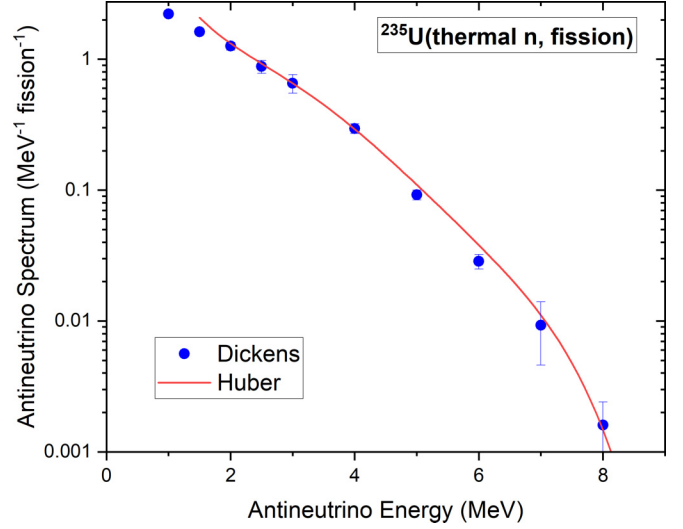


FIG. 2. Comparison between the Dickens and Huber antineutrino spectrum following the thermal-neutron induced fission of ^{235}U .

the corresponding equilibrium spectrum as

$$S_{eq,i}^a = S_{m,i}^a + \sum (CFY_j^a - Y_{j,i}^a) S_j, \quad (2)$$

where $Y_{j,i}^a$ are the effective cumulative yields during the experiment. Assuming that the nuclear data in the network, such as fission yields, decay branching ratios, half-lives, and electron/antineutrino spectra are of high fidelity, we can replace the $\sum (CFY_j^a - Y_{j,i}^a) S_j$ term by $(S_{s,eq}^a - S_{s,i}^a)$, where $S_{s,i}^a$ is the summation spectrum calculated with the i -irradiation conditions. Therefore, the ratio between two spectra obtained this way would be

$$R_{ab,i,k} = \frac{S_{eq,i}^a}{S_{eq,k}^b} = \frac{S_{m,i}^a + S_{s,eq}^a - S_{s,i}^a}{S_{m,k}^b + S_{s,eq}^b - S_{s,k}^b}, \quad (3)$$

which can be written as

$$R_{ab,i,k} = \frac{S_{m,i}^a}{S_{m,k}^b} C_{ab,i,k}, \quad (4)$$

with

$$C_{ab,i,k} = \frac{1 + (S_{s,eq}^a - S_{s,i}^a)/S_{m,i}^a}{1 + (S_{s,eq}^b - S_{s,k}^b)/S_{m,k}^b}, \quad (5)$$

factored out to help us understand how different $R_{ab,i,k}$ would be from the ratio of measured spectra $S_{m,i}^a/S_{m,k}^b$.

Plots of the $C_{ab,i,k}$ term for the ^{235}U to ^{239}Pu equilibrium electron spectra ratio are given in Fig. 3 for the three ORNL irradiation conditions. We have used the fission yields from the JEFF-3.3 library [28], and alternatively, the decay data from JEFF-3.3 or an updated version of the ENDF/B-VIII.0 [49] one. For the short irradiation and energies lower than 5 MeV, this term is very close to unity and the differences between the two decay data libraries are minimal; at higher energies, fluctuations in $C_{ab,i,k}$ are due to statistical effects in the measured spectra. For the medium and long irradiations, correction factors are more important and reliance on the summation method is higher. We can understand this fact from Fig. 4,

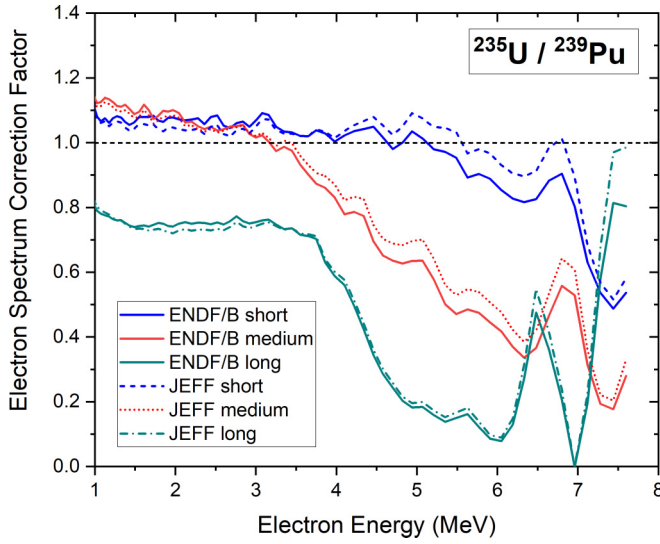


FIG. 3. Correction term needed to convert the measured ratio of ^{235}U to ^{239}Pu electron spectra to the corresponding spectra ratio under equilibrium conditions.

which shows $S_{s,i}^a/S_{s,eq}^a$ plots for the three ^{235}U irradiations. We can see that in the 1.5–7 MeV interval, the short irradiation accounts for 40–65% of the equilibrium spectrum, while the medium and long irradiations account for significantly less because of their considerably larger T_{cs} value.

The differences observed when using the JEFF-3.3 or ENDF/B-VIII.0 decay data are mainly due to the implementation of total absorption γ spectroscopy β intensities in the latter, see for instance Refs. [50–52]. This topic is explored in more detail in Fig. 5, which plots the ^{235}U electron spectrum measured at ILL divided by calculations that employ the JEFF-3.3 cumulative fission yields and alternatively the

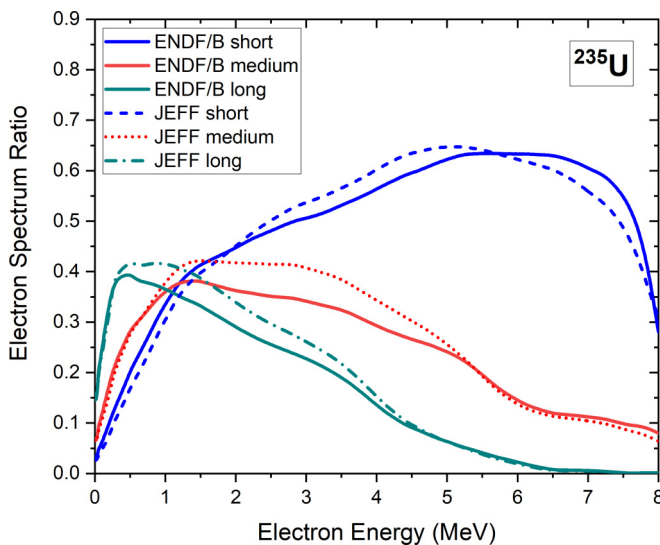


FIG. 4. Summation electron spectrum following the thermal neutron induced fission of ^{235}U under three different irradiation conditions, divided by the corresponding summation equilibrium spectrum.

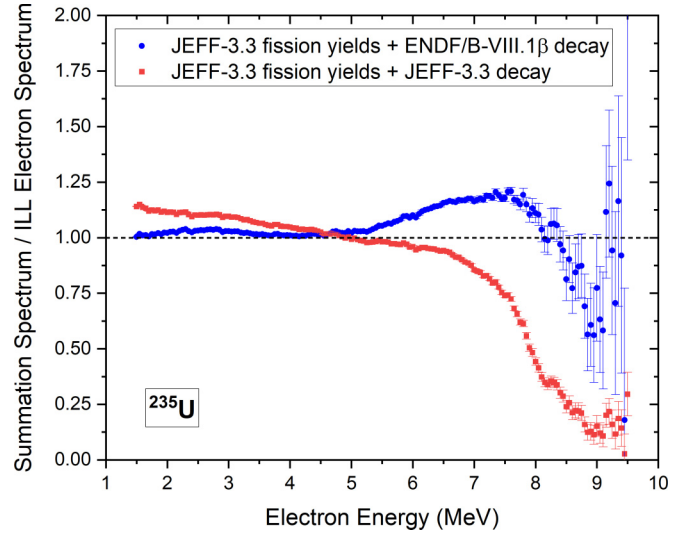


FIG. 5. Ratio of the ^{235}U electron spectrum measured at ILL to calculations using the JEFF-3.3 fission yields and alternatively the JEFF-3.3 or updated ENDF/B-VIII.0 decay data. Uncertainties are those from the ILL spectrum only.

JEFF-3.3 or updated ENDF/B-VIII.0 decay data. For energies less than 5 MeV, the ILL to JEFF decay ratio is larger than 1 due to the lack of TAGS beta intensities in it, while for energies higher than 6 MeV the ratio is considerably lower than 1 since the JEFF-3.3 decay data sublibrary does not contain theoretical electron spectra for fission products with incomplete decay data [53]. Similar results are observed for ^{239}Pu and ^{241}Pu .

Moving forward with our analysis, because of its small correction, the short irradiation results will be considered the most reliable of the three, and the updated ENDF/B-VIII.0 decay data will be used due to its higher fidelity in this particular application.

The $Y_{j,i}^a$ terms in Eq. (2) were obtained by numerically solving the corresponding Bateman's equations, which during the irradiation are

$$\frac{dN_j(t)}{dt} = R_f IFY_j - \lambda_j N_j + \sum b_{jk} \lambda_k N_k, \quad (6)$$

where R_f is the fission rate, while IFY_j , λ_j , and N_j are the independent fission yields, decay constant, and population for the j th fission product, and b_{jk} is the nuclear decay probability from the k th to the j th element in the decay network. After the irradiation, the term $R_f IFY_j$ disappears from this equation. Finally, $Y_{j,i}^a$ is obtained by integrating $N_j(t)$ during a specific counting interval

$$Y_{j,i}^a = N_f^{-1} \int N_j(t) dt, \quad (7)$$

where $N_f = \int R_f dt$, is the number of fission events during the irradiation.

As an example, the ORNL electron spectrum for the short irradiation on ^{239}Pu , with a waiting time of 19.7 s and a counting time of 5 s is compared with the corresponding $\sum Y_{j,i}^a S_j$ term in Fig. 6, highlighting also the most important contributors at 5 MeV of electron energy. Overall, the

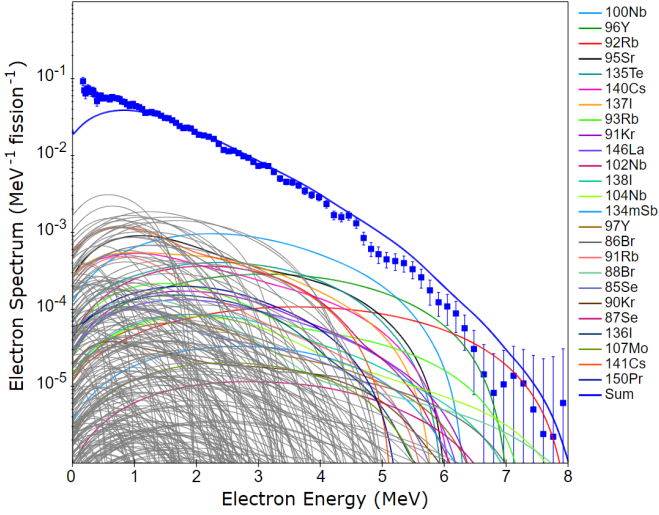


FIG. 6. Experimental and calculated ^{239}Pu electron spectra for the short irradiation, with a waiting time of 19.7 s and a counting time of 5 seconds. The contributions of the individual fission products are also plotted, and in particular, the largest contributors at 5 MeV are highlighted in color.

agreement between the ORNL electron data and the summation calculations is good; however, summation calculations tend to overestimate the sum spectra at the higher energies, with differences of up to 20%. We note that this disagreement has a negligible impact in the conclusions about the ILL normalizations drawn later in this paper.

Uncertainties in the $R_{ab,i,k}$ term will have experimental and databases contributions obtained as described below.

- (i) Uncertainties in the $(S_{s,eq}^a - S_{s,i}^a)$ terms are calculated using a Monte Carlo (MC) method, where for each history the independent fission yields, half-lives, decay branching ratios, and electron spectra were varied, leading to a new set of cumulative fission yields, and a new spectrum $S_{s,i}^a$ after solving the corresponding Bateman's equations; this approach validity was confirmed by calculating delayed neutron activities [54] mean values and standard deviations, which agreed well with evaluated ones [28].
- (ii) Since the experimental uncertainties $\Delta S_{m,i}^a$ are not available we derived them from the uncertainties of the individual spectra that are summed to obtain $S_{m,i}^a$, assuming that for electron energies larger than 1 MeV, spectra uncertainties are the sum of a statistical and a systematic term, $\Delta^2 S(E) = \Delta^2 S_{\text{stat}}(E) + \Delta^2 S_{\text{sys}}(E)$, with the former proportional to the square root of the spectrum, $\Delta S_{\text{stat}}(E) = c_{\text{stat}} S^{1/2}(E)$, and the latter proportional to the spectrum, $\Delta S_{\text{sys}}(E) = c_{\text{sys}} S(E)$. The c_{stat} and c_{sys} parameters were obtained from a fit to the approximately 700–900 $[S(E), \Delta S(E)]$ pairs of points per irradiation per target, with coefficients of determination R^2 values in the 0.74–0.98 range, noting that the long irradiation ^{241}Pu data accounts for the lower R^2 values; those c_{stat} and c_{sys} parameters were later used to obtain the $\Delta S_{m,i}^a$ values. As an

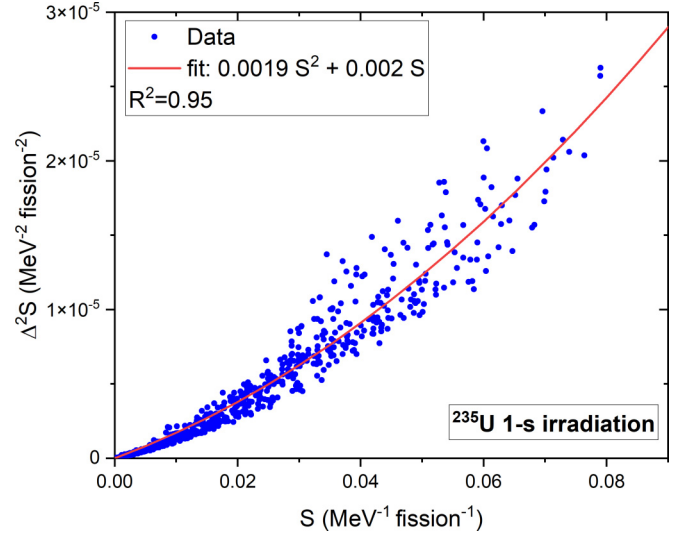


FIG. 7. Square of the electron spectrum uncertainty as function of electron spectrum for the short ^{235}U irradiation, including a quadratic fit to the data to obtain the uncertainty of the sum spectrum.

example, Fig. 7 shows the square of the electron spectrum uncertainties as function of spectrum values for the short ^{235}U irradiation, including the quadratic fit used to obtain the uncertainties in the sum spectrum.

- (iii) Experimental $\Delta S_{m,i}^a$ and MC $\Delta(S_{s,eq}^a - S_{s,i}^a)$ uncertainties were added in quadrature assuming no correlation between them.
- (iv) $\Delta R_{ab,i,k}$ were obtained employing a first-order Taylor expansion assuming no correlations between Eq. (3)'s numerator and denominator.

An interesting feature about Eq. (3) is that R_{aa} values for the three different possible irradiation combinations would provide a consistency check since they should be equal to unity. This is shown for the ratio of ^{235}U 's medium to short irradiation spectra in Fig. 8, with similar results for the other target and irradiation combinations. Consequently, we conclude that the most reliable energy range for our results is 1.5–5 MeV; for higher energies, uncertainties due to diminished statistics become dominant, not surprising in an experimental campaign designed to obtain β -decay heat values, which are proportional to $\int ES(E)dE$ with the integrand peaking in the 2–3 MeV region, rather than highly precise $S(E)$ values for energy values higher than 5 MeV.

VI. RESULTS

Results for the ^{235}U to ^{239}Pu electron spectra ratio (R_{59}) are given in Fig. 9, compared to the ILL and summation values, as well as the KI ones, the latter of which were read off the plot as the data were not made available. Figure 10 shows the ^{235}U to ^{241}Pu spectra ratio (R_{51}) results compared to the ILL and summation values, while results for the ^{241}Pu to ^{239}Pu spectra ratio (R_{19}) can be seen in Fig. 11. As mentioned earlier, our most reliable results are those from the short irradiation in the 1.5–5 MeV energy interval; despite their larger correction, results from the medium and long irradiation are also shown,

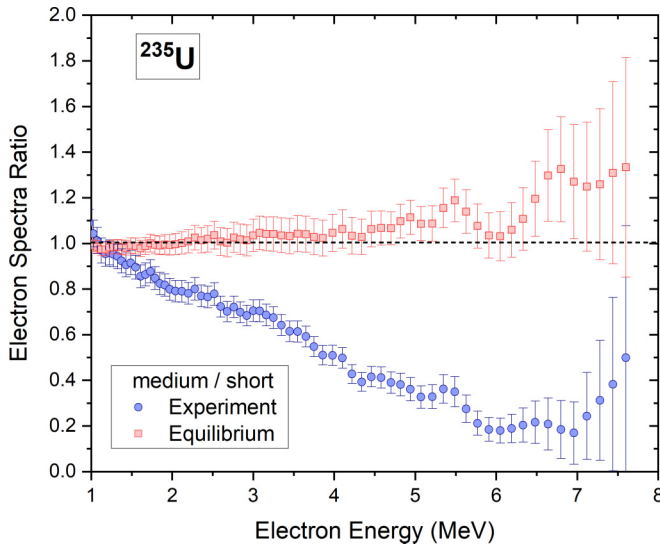


FIG. 8. Ratio of the experimental and equilibrium ^{235}U medium irradiation electron spectrum to the corresponding short one.

which will track closely with the summation results, particularly for energies larger than 3.5 MeV, where the correction factors are more dominant.

Overall, we observe differences with the ILL ratio values, and in particular (i) our R_{59} values align with the lower trend observed by Kopeikin *et al.* [31]; however, at around 3.5–4.5 MeV, where short irradiation corrections are minimal, our results are approximately halfway between the ILL and KI measurements. (ii) The ^{241}Pu electron spectrum seems larger than the ILL and summation results as evidenced by smaller R_{51} and larger R_{19} values. (iii) The ILL R_{51} values follow the summation calculations trend for higher energies, but the ILL R_{59} and R_{19} as well as KI R_{59} ones do not, which could indicate issues with the ^{239}Pu data at those energies; without attempting to provide an explanation, we nevertheless note

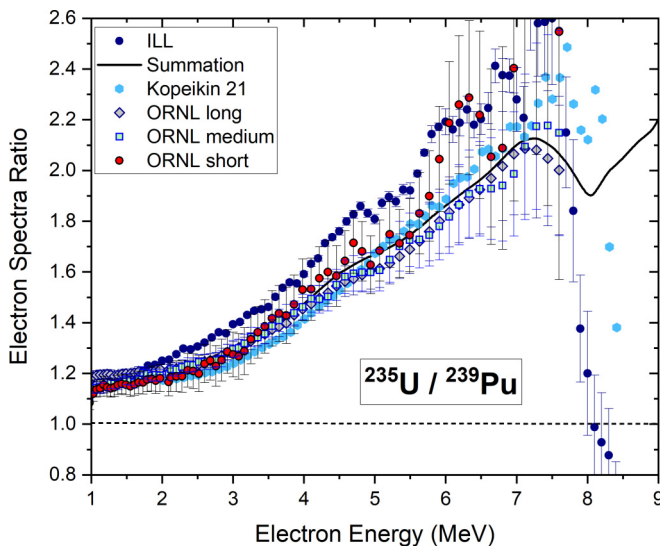


FIG. 9. Ratio of ^{235}U to ^{239}Pu electron spectra for thermal neutron-induced fission in equilibrium conditions.

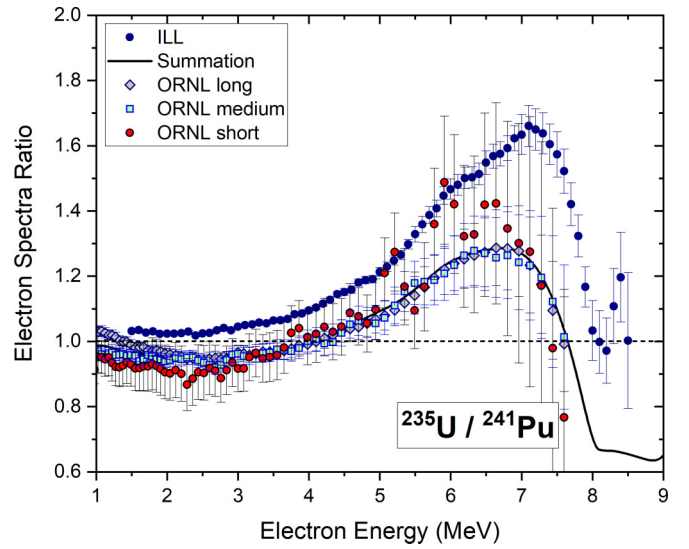


FIG. 10. Ratio of ^{235}U to ^{241}Pu electron spectra for thermal neutron-induced fission in equilibrium conditions.

that a small presence of ^{241}Pu or ^{235}U in the ^{239}Pu target could cause that behavior. Finally, we think that at this stage it is unlikely that we could use the ORNL data to normalize the ILL electron spectra to obtain new antineutrino spectra due to the lack of the ORNL sum spectra uncertainties and correlations.

Because of the lack of agreement between the R_{59} , R_{51} , and R_{19} values as shown in Figs. 9–11, it is clear that the best way forward would be to remeasure the electron spectra using an experimental technique employing the best features of the ILL, KI, and ORNL experiments, while minimizing nuclear databases' input. For precise normalization, counting of foils placed outside the reactor core would be needed, while for the measurement of the electron spectra, using detectors with

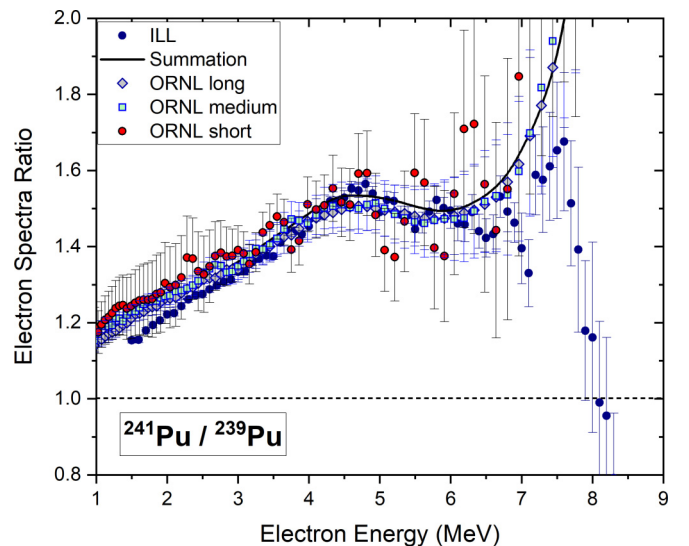


FIG. 11. Ratio of ^{241}Pu to ^{239}Pu electron spectra for thermal neutron-induced fission in equilibrium conditions.

superconducting solenoids, such as the one in Ref. [55], would be desirable since they would block γ rays and conversion electrons while providing superb energy resolution; in particular, the use of at least two of these detectors, with one counting at a fixed electron energy value, would define the spectrum's energy dependence even better. Additionally, a measurement of the ^{238}U electron spectrum at fast neutron energies using the same setup would be needed as the nuclear data behind the corresponding Mueller model [2] has been considerably improved and the only extant ^{238}U measurement [56] requires knowledge of the ^{235}U electron spectrum to deduce it. This experimental campaign would also yield precise values of the energies carried away by the antineutrinos, $\langle E_{\nu} \rangle$, to calculate the total energy released following fission [57,58], improve decay heat data [59], as well as help benchmark fission yield and nuclear decay databases.

VII. CONCLUSIONS

In summary, we have deduced the electron spectra ratio under equilibrium conditions R_{59} , R_{51} , and R_{19} from the electron spectra measured by Dickens *et al.* with the assistance of summation calculations that employ the latest nuclear databases. Our most reliable R_{59} values differ from the ILL ones and are in better agreement with those reported by Kopeikin *et al.*, supporting the hypothesis that the reactor antineutrino anomaly may be mainly due to faulty ^{235}U electron spectrum normalization. Additionally, our R_{19} values are also higher than those from ILL, indicating that the normalization for ^{239}Pu and ^{241}Pu may not be as precise as needed. These conclusions are supported by our survey of the ^{207}Pb thermal neutron cross-section data, with a recommended value lower

than the one used at ILL, and affecting the ^{235}U and ^{241}Pu ILL normalizations, as well as our assessment of the R_{59} behavior at high energies indicating a possible contamination in the ^{239}Pu target. As a consequence, we think that a new experimental campaign to measure electron spectra at a location that allows a precise normalization and using a spectrograph that provides high energy resolution and signal-to-noise ratio is needed to finally understand the electron antineutrino spectrum produced by nuclear reactors.

ACKNOWLEDGMENTS

Work at Brookhaven National Laboratory was sponsored by the U.S. Department of Energy, Office of Science, Office of Nuclear Physics under Contract No. DE-AC02-98CH10886, as well as by the U.S. Department of Energy, National Nuclear Security Administration, Office of Defense Nuclear Non-proliferation Research and Development (DNN R&D). We are grateful to Catherine Dunn for assistance in digitizing the ORNL reports tables. We acknowledge fruitful discussions with Krzysztof Rykaczewski, Charlie Rasco, Robert Grzywacz, Mitch Allmond, and Lowell Crow (ORNL), as well as Tibor Kibedi and Andrew Stuchbery (ANU) in preparation of the WoNDRAM workshop [60], which helped delineate our future experimental activities statements. We are also grateful to David Glasgow (ORNL) for guidance in trying to recover the full ORNL electron spectra data. Finally, our work on the $^{207}\text{Pb}(n, \gamma)$ cross section was motivated by discussions at the 2nd IAEA Technical Meeting on Nuclear Data Needs for Antineutrino Spectra Applications, organized by P. Dimitriou.

-
- [1] P. Huber, *Phys. Rev. C* **84**, 024617 (2011).
 [2] T. A. Mueller *et al.*, *Phys. Rev. C* **83**, 054615 (2011).
 [3] G. Mention, M. Fechner, Th. Lasserre, Th. A. Mueller, D. Lhuillier, M. Cribier, and A. Letourneau, *Phys. Rev. D* **83**, 073006 (2011).
 [4] F. P. An *et al.*, *Phys. Rev. Lett.* **116**, 061801 (2016).
 [5] Y. Abe *et al.*, *Phys. Rev. Lett.* **108**, 131801 (2012).
 [6] J. H. Choi *et al.*, *Phys. Rev. Lett.* **116**, 211801 (2016).
 [7] Y. Ko *et al.*, *J. Korean Phys. Soc.* **69**, 1651 (2016).
 [8] H. Almazan, L. Bernard, A. Blanchet, A. Bonhomme, C. Buck, P. Sanchez, I.E. Atmani, J. Haser, L. Labit, J. Lamblin, A. Letourneau, D. Lhuillier, M. Licciardi, M. Lindner, T. Materna, A. Minotti, A. Onillon, H. Pessard, J.S. Real, C. Roca, R. Rogly, T. Salagnac, V. Savu, S. Schoppmann, V. Sergeyeva, T. Soldner, A. Stutz, and M. Vialat, *Phys. Rev. Lett.* **125**, 201801 (2020).
 [9] J. Ashenfelter *et al.*, *Phys. Rev. Lett.* **122**, 251801 (2019).
 [10] F. P. An *et al.*, *Phys. Rev. Lett.* **128**, 081801 (2022).
 [11] H. Almazán *et al.*, *Phys. Rev. Lett.* **128**, 081802 (2022).
 [12] F. An *et al.*, *J. Phys. G: Nucl. Part. Phys.* **43**, 030401 (2016).
 [13] F. von Feilitzsch, A. A. Hahn, and K. Schreckenbach, *Phys. Lett. B* **118**, 162 (1982).
 [14] K. Schreckenbach *et al.*, *Phys. Lett. B* **160**, 325 (1985).
 [15] A. A. Hahn *et al.*, *Phys. Lett. B* **218**, 365 (1989).
 [16] L. Hayen, J. Kostensalo, N. Severijns, and J. Suhonen, *Phys. Rev. C* **99**, 031301(R) (2019).
 [17] A. Letourneau, V. Savu, D. Lhuillier, T. Lasserre, T. Materna, G. Mention, X. Mougeot, A. Onillon, L. Perisse, and M. Vivier, *Phys. Rev. Lett.* **130**, 021801 (2023).
 [18] F. P. An *et al.*, *Phys. Rev. Lett.* **118**, 251801 (2017).
 [19] D. Adey *et al.*, *Phys. Rev. Lett.* **123**, 111801 (2019).
 [20] S. F. Mughabghab, *Neutron Cross Sections*, Vol. 1, Neutron Resonance Parameters and Thermal Cross Sections, Part B, Z = 61–100 (Academic Press, New York, 1981).
 [21] E. T. Jurney and H. T. Motz, Argonne National Laboratory Report No. ANL-6797, 236, 1963.
 [22] D. Jowitt, S. K. Pattenden, H. Rose, V. G. Small, and R. B. Tattersall, United Kingdom Atomic Energy Research Establishment Report No. AERE R/R 2516, 1959.
 [23] S. F. Mughabghab, *Atlas of Neutron Resonances*, 6th ed. Vol. 2, Resonance Properties and Thermal Cross Sections Z = 61–102 (Elsevier, Amsterdam, 2018).
 [24] J. C. Blackmon, S. Raman, J. K. Dickens, R. M. Lindstrom, R. L. Paul, and J. E. Lynn, *Phys. Rev. C* **65**, 045801 (2002).
 [25] P. Schillebeeckx, T. Belgya, A. Borella, S. Kopecky, A. Mengoni, C. R. Quétel, L. Szentmiklósi, I. Trešl, and R. Wynants, *Eur. Phys. J. A* **49**, 143 (2013).
 [26] Applied Antineutrino Physics 2018 Workshop, <https://neutrinos.lnl.gov/workshops/aap2018>
 [27] A. Koning, R. Forrest, M. Kellett, R. Mills, H. Henriksson, and Y. Rugama, JEFF Report 21, Nuclear Energy Agency,

- Organisation for Economic Co-operation and Development, 2006.
- [28] A. J. M. Plompen *et al.*, *Eur. Phys. J. A* **56**, 181 (2020).
- [29] S. F. Mughabghab, *Atlas of Neutron Resonances*, 5th ed., Resonance Properties and Thermal Cross Sections $Z = 1-100$ (Elsevier, Amsterdam, 2005).
- [30] T. Kibédi Jr., T. W. Burrows, M. B. Trzhaskovskaya, P. M. Davidson, and C. W. Nestor, Jr., *Nucl. Instrum. Meth. Phys. Res. A* **589**, 202 (2008).
- [31] V. Kopeikin, M. Skorokhvatov, and O. Titov, *Phys. Rev. D* **104**, L071301 (2021).
- [32] F. P. An *et al.*, *Phys. Rev. Lett.* **129**, 041801 (2022).
- [33] J. K. Dickens, T. A. Love, J. W. McConnell, J. F. Emery, K. J. Northcutt, R. W. Peelle, and H. Weaver, ORNL Reports No. NUREG/CR-0162, 1978.
- [34] RSIC Data Library DLC-061, available from the Radiation Safety Information Computational Center (RSICC) at <https://rsicc.ornl.gov/codes/dlc/dlc0/dlc-061.html>.
- [35] J. K. Dickens, T. R. England, T. A. Love, J. W. McConnell, J. F. Emery, K. J. Northcutt, and R. W. Peelle, ORNL Reports No. NUREG/CR-1172, 1980.
- [36] J. K. Dickens, J. F. Emery, T. A. Love, J. W. McConnell, K. J. Northcutt, R. W. Peelle, and H. Weaver, ORNL Reports No. NUREG/CR-0171, 1978.
- [37] Justin Kirk Dickens, 1931–2013, ORNL employee from 1962–2002, <https://obituaries.goshennews.com/obituary/kirk-dickens-717029391>.
- [38] J. K. Dickens, T. A. Love, J. W. McConnell, and R. W. Peelle, *Nucl. Sci. Eng.* **74**, 106 (1980).
- [39] J. K. Dickens, T. A. Love, J. W. McConnell, and R. W. Peelle, *Nucl. Sci. Eng.* **78**, 126 (1981).
- [40] B. Pritychenko, E. Betak, M. A. Kellett, B. Singh, and J. Totans, *Nucl. Instrum. Meth. Phys. Res. A* **640**, 213 (2011).
- [41] N. Otuka *et al.*, *EPJ Web Conf.* **239**, 15001 (2020).
- [42] M. Akiyama and S. An, in *Proceedings of the International Conference on Nuclear Data for Science and Technology, Antwerp, 1982*, edited by K. H. Bockhoff (D. Reidel Publishing Company, Holland, 1983), p. 237.
- [43] N. Hagura, T. Yoshida, and T. Tachibana, *J. Nucl. Sci. Technol.* **43**, 497 (2006).
- [44] J. K. Dickens, *Phys. Rev. Lett.* **46**, 1061 (1981).
- [45] P. Vogel, G. K. Schenter, F. M. Mann, and R. E. Schenter, *Phys. Rev. C* **24**, 1543 (1981).
- [46] A. A. Sonzogni, T. D. Johnson, and E. A. McCutchan, *Phys. Rev. C* **91**, 011301(R) (2015).
- [47] M. Estienne *et al.*, *Phys. Rev. Lett.* **123**, 022502 (2019).
- [48] K.-H. Schmidt, M. Estienne, M. Fallot, S. Cormon, A. Cucoanes, T. Shiba, B. Jurado, K. Kern, and Ch. Schmitt, *Nucl. Data Sheets* **173**, 54 (2021).
- [49] D. A. Brown *et al.*, *Nucl. Data Sheets* **148**, 1 (2018).
- [50] R. C. Greenwood, R. G. Helmer, M. H. Putnam, and K. D. Watts, *Nucl. Instrum. Methods Phys. Res., Sect. A* **390**, 95 (1997).
- [51] A. Algora *et al.*, *Phys. Rev. Lett.* **105**, 202501 (2010).
- [52] B. C. Rasco *et al.*, *Phys. Rev. Lett.* **117**, 092501 (2016).
- [53] T. Kawano, P. Moller, and W. B. Wilson, *Phys. Rev. C* **78**, 054601 (2008).
- [54] P. Dimitriou *et al.*, *Nucl. Data Sheets* **173**, 144 (2021).
- [55] A. A. Aava, P. Jones, I. T. Usman, M. V. Chisapi, T. Kibedi, B. R. Zikhali, and L. Msebi, *Nucl. Instrum. Meth. Phys. Res. A* **964**, 163809 (2020).
- [56] N. Haag, A. Gutlein, M. Hofmann, L. Oberauer, W. Potzel, K. Schreckenbach, and F. M. Wagner, *Phys. Rev. Lett.* **112**, 122501 (2014).
- [57] V. I. Kopeikin, L. A. Mikaelyan, and V. V. Sinev, *Phys. Atom. Nucl.* **67**, 1892 (2004).
- [58] X. B. Ma, W. L. Zhong, L. Z. Wang, Y. X. Chen, and J. Cao, *Phys. Rev. C* **88**, 014605 (2013).
- [59] A. L. Nichols, P. Dimitriou, A. Algora, M. Fallot, L. Giot, F. G. Kondev, T. Yoshida, M. Karny, G. Mukherjee, B. C. Rasco, K. P. Rykaczewski, A. A. Sonzogni, and J. L. Tain, *Eur. Phys. J. A* **59**, 78 (2023).
- [60] C. Romano, N. Bowden, A. Conant, B. Goldblum, P. Huber, J. Link, B. Littlejohn, H. P. Mumm, J. Ochoa, S. Prasad, C. Riddle, A. Sonzogni, and W. Wieselquist, Lawrence Livermore National Laboratory Report LLNL-TR-829851, 2021.